Inorganic Chemistry

Article

pubs.acs.org/IC

Electrochemical Water Oxidation by *In Situ*-Generated Copper Oxide Film from $[Cu(TEOA)(H_2O)_2][SO_4]$ Complex

Ting-Ting Li,[†] Shuang Cao,[†] Chao Yang,[‡] Yong Chen,[†] Xiao-Jun Lv,[†] and Wen-Fu Fu*[,†,‡]

[†]Key Laboratory of Photochemical Conversion and Optoelectronic Materials and HKU-CAS Joint Laboratory on New Materials, Technical Institute of Physics and Chemistry and University of Chinese Academy of Sciences (CAS), Beijing 100190, People's Republic of China

[‡]College of Chemistry and Engineering, Yunnan Normal University, Kunming 650092, People's Republic of China

Supporting Information

ABSTRACT: Although many noble-metal oxide catalysts show high activities and low overpotentials for water oxidation, there remain challenges in the sustainable developments of more inexpensive, efficient, and robust catalysts. Here, we report a heterogeneous copper oxide film toward water oxidation formed upon the oxidative polarization of an acetate electrolyte containing Earth-abundant Cu(II) salts in combination with commercially available triethanolamine (TEOA) as the catalyst precursor. A 1:1 molar ratio of TEOA coordinates to Cu(II) is favored in aqueous solution and the single crystal of the complex was obtained. The film has a modest overpotential of 550 mV and the catalytic performance of the material is demonstrated by long-term electrolysis at 1.3 V vs normal hydrogen electrode, a stable current density persists for at least 3 h, and a Faradaic efficiency of almost 100% is obtained.

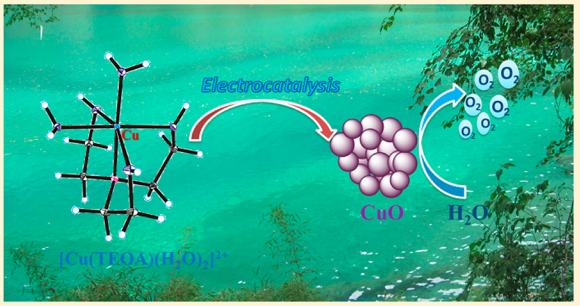

INTRODUCTION

Hydrogen has been proposed as an ideal energy store, because of its high energy density and the formation of water as the sole product of combustion.[1] Clean hydrogen fuel may improve the usability of renewable energy sources, and it can be produced through water splitting.[2] Water splitting involves two half-reactions: a reduction of water to hydrogen, and an oxidation of water to oxygen. The latter is considered as the bottleneck in the overall water splitting process. The four-electron oxidation of two water molecules, coupled with the removal of four protons to form a new O−O bond, is a complex endothermic transformation.[3] In nature, water oxidation occurs in Photosystem II (PSII) by a proton-coupled electron transfer (PCET) process where the oxygen-evolving catalyst, a $CaMn_4O_5$ cluster, is converted to a high-valent metal-oxo species, which, in turn, generates dioxygen.[4] Inspired by natural photosynthesis, many functional catalysts for water oxidation have been developed through the utility of transition metals that can undergo multiple oxidation or reduction states. Although molecular and precious metal oxide catalysts[5] such as Ru and Ir feature low overpotentials and high turnover rates in water oxidation, it is not preposterous to exploit more abundant, environmentally benign, and inexpensive transition metals. First-row transition metals, such as cobalt,[6] iron,[7] manganese,[8] and nickel,[9] are of particular interest for water oxidation catalysts (WOCs). Copper is a well-known catalyst for oxidizing organic compounds such as phenols, alcohols, and even hydrocarbons,[10] but its use in water oxidation has been explored in much less detail than other first-row transition metals. Recently, a handful of homogeneous copper-based WOCs have been reported including Cu(II) polypeptide complex,[11] Cu(II) 2,2′-bipyridine[12] and Cu(II) salt systems containing neutral to weakly basic aqueous buffers,[13] a biomimetic Cu(II) system with 6,6′-dihydroxy-2,2′-bipyridine ligand,[14] as well as Cu^{II}-(Py_3P), where Py_3P is *N*,*N*-bis(2-(2-pyridyl)ethyl) pyridine-2,6-dicarboxamidate.[15] These above-mentioned Cu-based molecular catalysts could access high-oxidation-state copper intermediates that can generate oxygen under modest overpotentials. However, it would be highly desirable to develop heterogeneous Cu-based WOCs, because of their tunable properties and greater durability. Du and co-workers reported an *in situ*-generated nanostructured CuO film from bulk electrolysis of copper 2-pyridylmethylamine complex is active for water oxidation.[16] In addition, a robust water oxidation catalyst based on copper oxide was electrodeposited from borate buffer solution containing Cu(II) salts.[17]

Herein, we reported a copper oxide film that behaves as an electrocatalyst for water oxidation. The film was electrodeposited from a basic electrolyte containing molecular $[Cu(TEOA)(H_2O)_2][SO_4]$ complex. The deposited film was robust and showed electrocatalytic activity for water oxidation with almost 100% Faradaic efficiency. Its morphology and composition were investigated by scanning electron microscopy (SEM), energy-dispersive X-ray (EDX) spectroscopy, and X-ray

Received: February 5, 2015
Published: February 25, 2015

DOI: 10.1021/acs.inorgchem.5b00266
Inorg. Chem. 2015, 54, 3061−3067

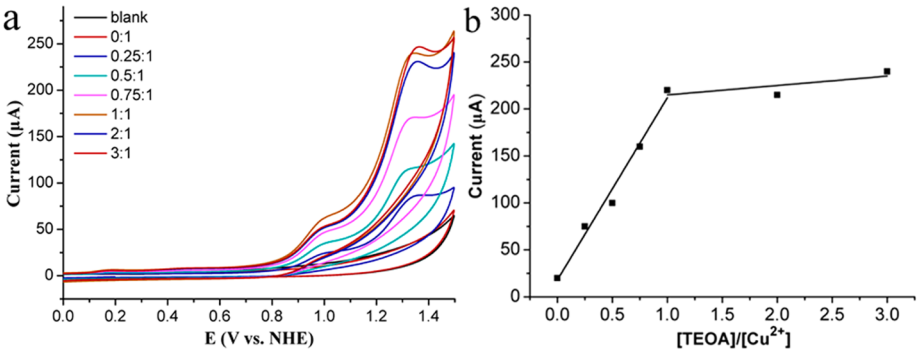

Figure 1. (a) CV measured at various TEOA concentrations and (b) plot of the catalytic current at 1.30 V vs NHE against the TEOA:Cu molar ratio.

photoelectron spectroscopy (XPS), as well as inductively coupled plasma−mass spectrometry (ICP-MS).

EXPERIMENTAL SECTION

Materials and Instrumentations. $CuSO_4·5H_2O$, triethanolamine (TEOA), triethylamine (TEA), NaOAc, Na_2CO_3, NaH_2PO_4, Na_2HPO_4, $Na_2B_4O_7·10H_2O$, NaCl, and other chemicals were commercially available without further purification. All aqueous solutions were prepared with Milli-Q ultrapure water (>18 MΩ) unless stated otherwise. The pH value of the electrolyte was adjusted by 0.1 M NaOH. Indium tin oxide (ITO) conducting glasses were purchased from Dalian Heptachroma Company (thickness ∼1.0 mm, transmittance >85%, resistance ∼12 Ω).

Cyclic voltammetry (CV), which involves controlled potential electrolysis (CPE), were carried out on a Shanghai Chenhua Model CHI660C electrochemical potentiostat. The three electrodes system consisted of a working electrode, a platinum slice counter electrode, and an Ag/AgCl reference electrode (∼0.199 V vs normal hydrogen electrode (NHE)). Diffuse reflectance spectra and absorption spectrum were recorded on a Hitachi Model UV-3010 spectrophotometer. SEM images and EDX spectra were obtained on a Hitachi Model S-4800 scanning electron microscope. Powder X-ray diffraction (PXRD) patterns were collected by using a Bruker D8 Focus with Cu Kα radiation at (λ = 1.54056 Å). pH values were measured by using a Model pH S-3C meter (Mettler−Toledo FE20, China). XPS data were obtained by using an ESCALa-b220i-XL electron spectrometer (VG Scientific), using 300 W Al Kα radiation. The binding energies were obtained with reference to the C 1s line at 284.8 eV. The analysis of the deposited film was carried out using ICP-MS (NexION 300X, Perkin−Elmer).

Electrode Pretreatment. Prior to experiments, the indium tin oxide (ITO) glass slides (1.0 cm × 2.0 cm) were cleaned by sonication in acetone and Milli-Q ultrapure water for ∼20 min respectively, followed by drying at room temperature for ∼30 min. They were stored in airtight glass bottle before use. The glassy carbon electrode (0.07 cm^2) was successively polished with 3.0 and 1.0 mm diamond pastes and sonicated in Milli-Q ultrapure water before use.

Electrochemical Measurements. In a homogeneous system, the CVs were recorded in acetate electrolyte (pH 12.4, 0.1 M), except as otherwise noted. The glassy carbon, or ITO, was used as the working electrode, Ag/AgCl electrode (3.0 M KCl) as the reference electrode, platinum slice as the counter electrode. The CV scans were recorded in a range of 0−1.5 V under an argon atmosphere with a scan rate of 100 mV/s. The CPE for homogeneous system was performed in a gas-tight two-compartment electrochemical cell with a glass frit junction, and the potential was fixed at 1.3 V vs NHE without *iR* compensation. The counter electrode was charged with 20 mL acetate electrolyte, and the working electrode (ITO) and reference electrode were charged with 20 mL of electrolyte containing 2.0 mM $[Cu(TEOA)(H_2O)_2][SO_4]$ complex. The CPE for heterogeneous system was conducted using a homemade electrochemical cell in acetate electrolyte without $[Cu(TEOA)(H_2O)_2][SO_4]$ complex. Prior to experiments, the electrolyte was degassed by bubbling with high purity Ar for 30 min with vigorous stirring.

Oxygen Evolution and Faradaic Efficiency Calculation. For CPE, the generated oxygen in the headspace was monitored by an Ocean Optics optical probe and was quantified by gas chromatography (GC) on a Shimadzu Model GC-2014 instrument equipped with a 5 Å molecular sieve column (3.0 m × 2.0 mm), a thermal conductivity detector and argon carrier gas. The theoretical amount of evolved oxygen is calculated according to the recorded passed charge using Faraday's law, with a Faradaic efficiency (FE) of

$$\mathrm{FE}\,(\%) = \frac{n_{\mathrm{meas\ O_2}}}{n_{\mathrm{calcd\ O_2}}} \times 100$$

X-ray Crystallography. A single crystal of the $[Cu(TEOA)(H_2O)_2][SO_4]$ was obtained by slow diffusion of diethyl ether into a mixed solution (1:1, v/v water/methanol) containing $CuSO_4$ and excess TEOA. Diffraction data were collected on a Rigaku Model Saturn724 CCD diffractometer using a graphite monochromator with Mo Kα radiation (λ = 0.071073 nm) at 113 K. The molecular structure of the prepared complex was resolved by direct methods and refined by full-matrix least-squares methods on all $F2$ data (SHELXL-97). Non-hydrogen atoms were refined anisotropically. The position of the hydrogen atoms was calculated and refined isotropically.[18] CCDC Reference No. 948349 contains the supplementary crystallographic data for $[Cu(TEOA)(H_2O)_2][SO_4]$. These data can be obtained free of charge from The Cambridge Crystallographic Data Centre via www.ccdc.cam.ac.uk/data_request/cif.

RESULTS AND DISCUSSION

Electrochemical Properties of Cu(II)/TEOA Solution. TEOA has been previously used as a multidentate ligand in several metal complexes.[19] The hydroxyl coordination sites of the metal may be involved in the catalytic water oxidation cycle, lowering the water oxidation overpotential.[14a] Figure 1a showed changes in the cyclic voltammetry (CV) of a 1.0 mM $CuSO_4$ solution with 0.1 M acetate electrolyte at pH 12.4, as various amounts TEOA were added. The CV scans were recorded using a glassy carbon working electrode (diameter: 3.0 mm) under an argon atmosphere. The reference electrode was Ag/AgCl with potentials reported versus NHE by the addition of 0.199 V to the measured potentials. Upon scanning at 100 mV/s from 0 to 1.5 V, the voltammogram exhibited a single oxidation wave at E_{pa} = 0.97 V, which was assigned to the ligand oxidation peak (see Figure S1 in the Supporting Information). At more positive potentials, an irreversible oxidation wave with an onset potential of E_{pa} = 1.05 V appeared with a greatly enhanced catalytic current compared with that of the solution without the catalyst (black line in Figure 1a). Scanning this solution in the cathodic direction, the first time, showed one

DOI: 10.1021/acs.inorgchem.5b00266
Inorg. Chem. 2015, 54, 3061−3067

irreversible reduction peak at E_{pc} = −0.23 V (see Figure S2 in the Supporting Information), which was attributed to $Cu^{II/I}$ reduction wave.[20] Among the electrochemical window, a new reduction peak appeared at E_{pc} = −0.35 V and the intensity of the peak increased proportionally with scan time (see Figure S3 in the Supporting Information). The cathodic wave was attributed to the O_2/O_2^- couple, indicating that the water oxidation had occurred. The observed overpotential of 550 mV is slightly lower than that of previously reported Cu-based molecular catalysts.[11−13] Additionally, Figure 1b showed that the addition of TEOA increased the catalytic current measured at 1.30 V, to a maximum of ∼250 μA at a 1:1 molar ratio. The current then became independent of the TEOA concentration above 1.0 mM, which demonstrated that a 1:1 stoichiometry TEOA/Cu yields the maximum response. In contrast, a solution containing only 1.0 mM Cu(II) salt with anion of SO_4^{2-}, NO_3^{2-}, OAc^-, or Cl^- at pH 12.4 immediately formed a precipitate of $Cu(OH)_2$ ($K_{sp} = 2.0 \times 10^{-19}$)[21] and the resulting suspension had no activity toward water oxidation (red line in Figure 1a). Furthermore, upon addition of TEA to the above solution, the suspension remained and no catalytic current was observed. Taken together, these results indicate the occurrence of water oxidation can be attributed to the Cu(II) complex with TEOA ligand rather than free Cu(II) in solution.

Structural Studies and Electrochemistry of [Cu(TEOA)-$(H_2O)_2$][SO_4]. Encouraged by the catalytic efficiency of the solution based on a $CuSO_4$/TEOA (1:1) system, we investigated the crystal structure of the complex by XRD analysis. Small cubelike crystals suitable for X-ray structure determination were obtained by vapor diffusion of diethyl ether into a mixed solution (1:1, v/v water/methanol) containing $[Cu(TEOA)(H_2O)_2][SO_4]$. The complex cation $[Cu(TEOA)(H_2O)_2]^{2+}$ features an octahedral geometry around the Cu atom with one quadridentate TEOA ligand and two water molecules. TEOA occupies four coordination sites binding through three hydroxyls and one tertiary amine group with one water molecule located in the equatorial plane and another in an axial position (see Figure 2 and Table S1 in the Supporting Information). These results confirm that a 1:1 ratio of Cu(II) coordinate to TEOA is favored in aqueous solution,[20b] presumably because of the chelation effect of TEOA and low steric hindrance of the water molecules. The UV-vis absorption spectra of $CuSO_4$/TEOA (1:1) and the $[Cu(TEOA)(H_2O)_2][SO_4]$ complex in an acetate electrolyte (0.1 M, pH 12.4) showed the presence of same species in basic aqueous solution (see Figure S4 in the Supporting Information). The band observed at 690 nm is characteristic of Cu(II) center d−d transitions.

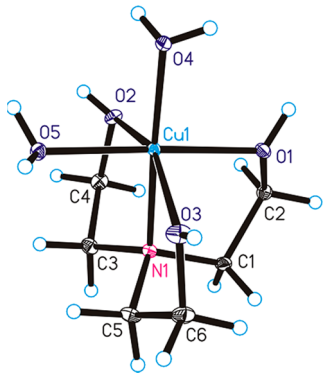

Figure 2. Perspective view and labeling scheme for $[Cu(TEOA)(H_2O)_2]^{2+}$ cation, the SO_4^{2-} anion was omitted for clarity. Selected bond lengths: Cu1−O1, 1.99(1) Å; Cu1−O2, 2.39(1) Å; Cu1−O3, 2.29(1) Å; Cu1−O4, 1.94(1) Å; Cu1−O5, 1.999(5) Å. Selected bond angles: O1−Cu1−O2, 92.07(4)°; O1−Cu1−O3, 93.01(4)°; O1−Cu1−O4, 93.02(4)°; O1−Cu1−O5, 176.92(4)°; O2−Cu1−O3, 157.25(4)°; O2−Cu1−O4, 100.09(4)°; O2−Cu1−O5, 85.94(4)°; O3−Cu1−O4, 101.77(4)°; O3−Cu1−O5, 87.96(4)°; O4−Cu1−O5, 89.64(4)°; N1−Cu1−O1, 83.86(4)°; N1−Cu1−O2, 77.91(4)°; N1−Cu1−O3, 80.60(4)°; N1−Cu1−O4, 176.20(4)°; and N1−Cu1−O5, 93.43(4)°.

Electrochemical properties of the obtained Cu(II) complex were carried out. The results demonstrated that the catalytic current of the peak at E_{pa} = 1.30 V varied linearly with $[Cu(TEOA)(H_2O)_2][SO_4]$ concentration and yielded a maximum current of 400 μA at 2.0 mM, indicating single-site copper catalysis behavior (see Figure S5 in the Supporting Information). At higher concentrations (>2.0 mM), the current became independent of a catalyst concentration and was limited by both substrate diffusion and the reaction kinetics.

Homogeneous or Heterogeneous Catalyst? It is important to determine if metal complexes remain unchanged or act as precursors of a true active species during catalysis, as has been found for some single site Co,[22] Ir,[23] and Fe[24] complexes. We performed CV and bulk electrolysis over an extended period to assess possible changes in this system. CV cycles 10 times showed an increase in amplitude of the peak current and a change of the wave shape (Figure 3a). Following these scans, the working electrode was rinsed in water and then cycled in fresh electrolyte without catalyst. The observed CV in fresh electrolyte was nearly the same as that observed in $[Cu(TEOA)(H_2O)_2][SO_4]$ solution. However, after polishing the electrode, no catalytic response was observed in the catalyst-free electrolyte (Figure 3b). A similar phenomenon was observed when the glassy carbon electrode was replaced by an ITO working electrode (see Figure S6 in the Supporting Information). Controlled potential electrolysis was performed in a gas-tight two-compartment electrochemical cell with a glass frit junction and the potential fixed at 1.30 V vs NHE without *iR* compensation. The working electrode (ITO, 1.0 cm^2) and reference electrode were charged with 20 mL of electrolyte containing 2.0 mM $[Cu(TEOA)(H_2O)_2][SO_4]$ complex. The counter electrode was charged with another 20 mL of acetate electrolyte. Evolution of O_2 was monitored by a fluorescence oxygen probe (Ocean Optics) and quantified by gas chromatographic (Shimadzu, Model GC-14C) analysis. Figure 4 demonstrated that the catalytic current was sustained for at least 5 h at a stable current density of 1.6 mA/cm^2. Under these conditions, nearly 60.0 μmol of O_2 were produced with a Faradaic efficiency of ca. 80.0% (see Figure S7 in the Supporting Information). This equates to a catalytic turnover number (TON) of ∼1.5, based on the initial catalyst concentration of the solution. It is not surprising that we got low TON values, since only electrode surface contacted catalysts are expected to be responsible for catalysis. Conversely, when electrolysis was carried out during the absence of catalyst, no catalytic current was observed (red line in Figure 4).

During electrolysis, a brown film became apparent on the ITO electrode that darkened over the extended electrolysis period. The surface deposits also appeared even when the concentration of the catalyst was decreased to 0.5 mM. The film was insoluble in organic solvents and in basic aqueous solution with pH > 12.4. The CV scans of the film were

DOI: 10.1021/acs.inorgchem.5b00266
Inorg. Chem. 2015, 54, 3061−3067

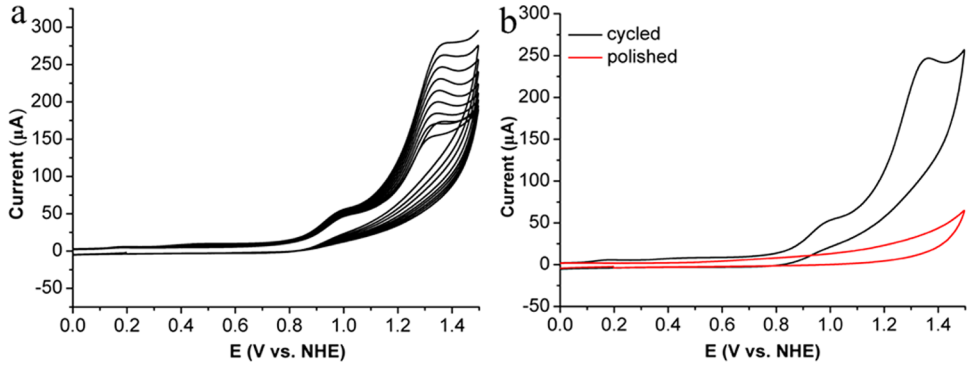

Figure 3. (a) Successive CV cycles with 2.0 mM $[Cu(TEOA)(H_2O)_2][SO_4]$ at a glassy carbon electrode in an acetate electrolyte (0.1 M) at pH 12.4, 100 mV/s scan rate. (b) CV response after multiple scans for a polished (red line) and rinsed (black line) working electrode in a fresh acetate electrolyte without catalyst.

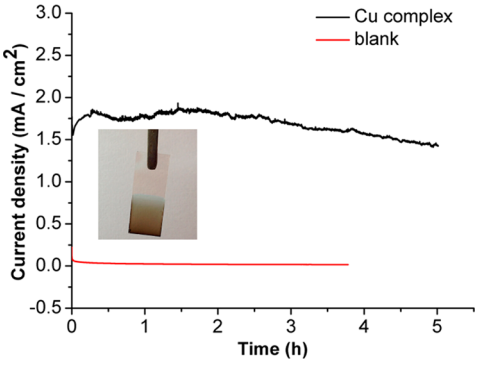

Figure 4. CPE without (red line) and with (black line) 2.0 mM $[Cu(TEOA)(H_2O)_2]SO_4$ at an ITO (1.0 cm^2) electrode in acetate electrolyte (0.1 M) at pH 12.4 and 1.30 V vs NHE. The inset showed an image of the brown film obtained after 5 h of bulk electrolysis.

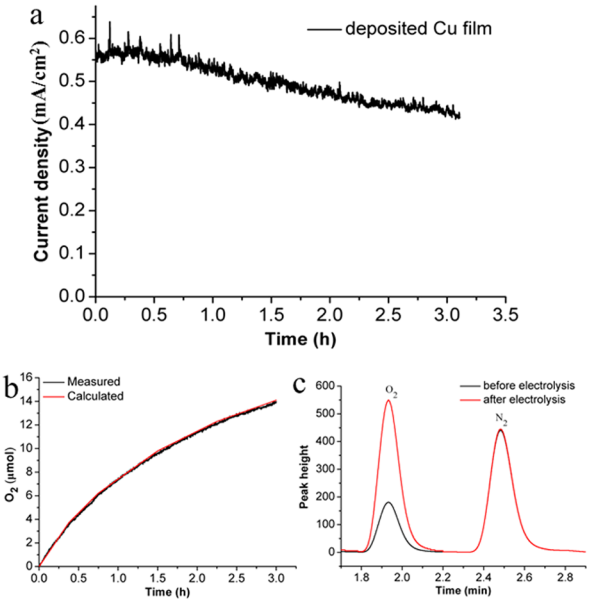

Figure 5. (a) CPE of the deposited film in an acetate electrolyte (0.1 M) at pH 12.4 and 1.30 V vs NHE. (b) O_2 production measured by fluorescent oxygen probe (black line) and calculated amount of O_2 produced (red line). (c) Gas chromatography trace before (black line) and after (red line) electrolysis (N_2 peaks completely overlap).

reproducible over 100 successive reverse scan cycles and displayed a broad cathodic feature at 0.85 V, which was assigned to a reduction of the surface-deposited species (see Figure S8 in the Supporting Information). Only a slight decrease in catalytic current was observed over repeated cycles indicating the robustness of the film. To further verify the catalytic performance of the deposited films, CPE was conducted in a closed, deoxygenated electrolysis cell at 1.30 V. A stable current density of 0.55 mA/cm^2 was achieved and retained more than 80% of its maximum value after an electrolysis period of 3 h (Figure 5a). This decrease may be attributed to the combination of decreased electrolyte pH and gradual peeling of the film from the ITO surface. A total of 14.0 μmol O_2 was achieved and the Faradaic efficiency was calculated to be almost 100%, based on the total charge that flowed (Figure 5b). A previous report of Cu(II) salt catalysis by Meyer,[13] suggested that a precipitated film could form on an ITO electrode at high initial Cu(II) salt concentrations (>2.0 mM), but the solid redissolved into the electrolyte over 10−15 min. By contrast, in this study, the surface deposits appeared even at a low $[Cu(TEOA)(H_2O)_2][SO_4]$ concentration of 0.5 mM, and remained stable for least 3 h of bulk electrolysis. This highlights the robustness of this heterogeneous electrocatalyst.

The current density (j) for O_2 evolution achieved for the deposited film was measured at a variety of applied potentials. An appreciable catalytic current was observed beginning at an overpotential (η) of 0.45 V. A Tafel plot of log(j) versus η depicted in Figure 6, shows a slope of −130 mV/decade in the range of 0.45−0.60 V. The Tafel plot deviated slightly from linearity at high η possibly because of the uncompensated iR drop on the surface of the ITO electrode.

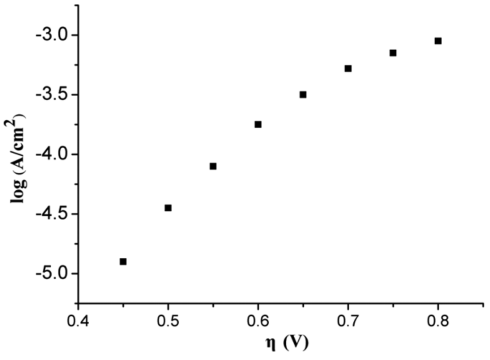

Figure 6. Tafel plot of the fresh prepared film in an acetate electrolyte (0.1 M) at pH 12.4. $\eta = V_{appl} - iR - E^0$.

DOI: 10.1021/acs.inorgchem.5b00266
Inorg. Chem. 2015, 54, 3061−3067

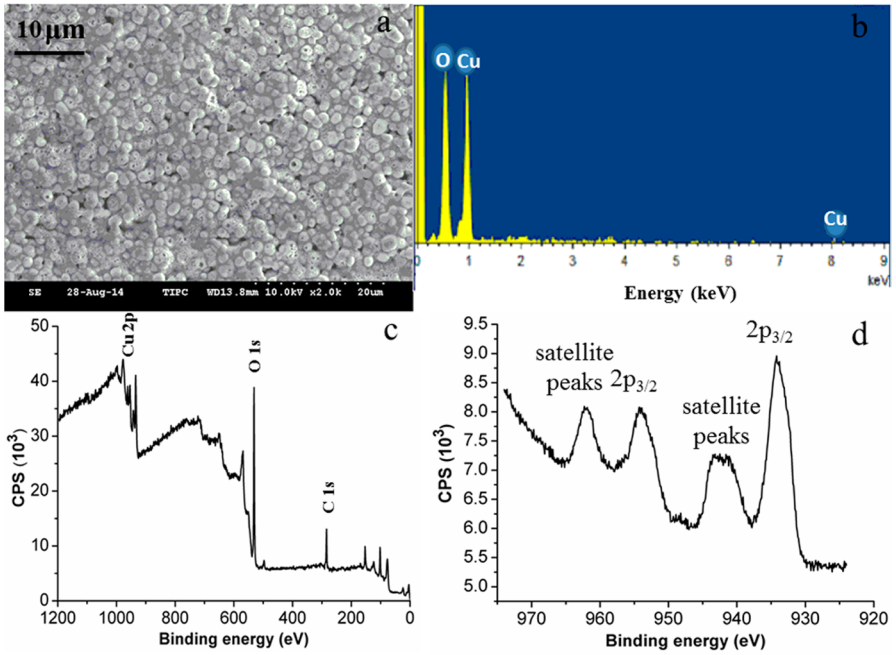

Figure 7. (a) SEM image of the film deposited on ITO at 1.30 V for 5 h in an acetate electrolyte (0.1 M) at pH 12.4. (b) EDX spectrum of the film deposited on the surface of the ITO. (c) XPS survey scans of the film, the binding energies were obtained with reference to the C 1s line at 284.8 eV. (d) High-resolution XPS scan centered on the Cu 2p peak.

The appropriate choice of buffer/electrolyte and pH range is critical for electrocatalytic water oxidation. There are similar reports of heterogeneous catalysts such as Co-Pi,[25] Co-Bi,[26] and Ni-Bi[9a] that can only form in proton-accepting electrolytes. Even in Sun's system, the copper oxide thin film was formed in a borate electrolyte.[17] Significantly, the formation of the electrocatalytic film in our work also proceeded in a 0.1 M NaCl electrolyte (pH adjusted to 12.4 via the addition of 0.1 M NaOH) containing 2.0 mM $[Cu(TEOA)(H_2O)_2][SO_4]$ (see Figure S9 in the Supporting Information). However, the current density of the film rapidly dropped from 1.6 to below 0.25 mA/cm^2, when the electrolyte was replaced by fresh NaCl without complex (see Figure S10 in the Supporting Information). We tentatively suggested that, in the case of the former, the presence of $[Cu(TEOA)(H_2O)_2][SO_4]$ prevents the film from peeling off. In contrast, the generated films in Na_2CO_3 or $H_2BO_3^-/H_3BO_3$ electrolytes displayed sustained catalytic water oxidation activity and maintained current densities above 2.0 mA/cm^2 in the presence or absence of catalyst precursor, which highlights the robustness of this heterogeneous electrocatalyst (see Figures S11−S14 in the Supporting Information). These results, when taken together, indicate proton-accepting electrolytes play the crucial role of enhancing film stability and improve catalytic efficiency in this system.

Characterization of Film. The robust catalytic activity of the deposited film toward water oxidation compelled us to study its morphology, composition, and structure. The diffuse reflectance spectrum of the film (see Figure S15 in the Supporting Information) showed absorption features at λ_{max} = 375 and 590 nm, along with obvious broad bands in the visible region. First, the morphology of the film was characterized by SEM and PXRD. Figure 7a showed the film consists of micrometer-sized particles on surface of ITO. The PXRD patterns only showed the peaks associated with the ITO character, and they revealed that this film is amorphous (see Figure S16 in the Supporting Information). The composition and the chemical states of the amorphous film were further analyzed by EDX and XPS, as well as ICP-MS. EDX spectra (Figure 7b) measured from several independently prepared films, showed that the films formed in acetate solution contained only Cu and O. Similar results were obtained from the films produced in the other buffer/electrolyte (see Figures S17−S19 in the Supporting Information). Although the morphology of the film was not well-suited for quantitative EDX, the Cu:O ratio was close to 1:1. The absence of C suggests that neither acetate nor the TEOA ligand were co-deposited during electrocatalysis. In addition, electrolysis was repeated on larger ITO electrodes, ICP-MS analysis of dried solid scraped off from ITO electrodes showed a O:Cu molar ratio of ∼1.0. Finally, the XPS spectral data in Figure 7c further verified the elemental composition of the films. High-resolution spectra of the characteristic peaks at 933.9 and 953.9 eV assigned to Cu $2p_{3/2}$ and $2p_{1/2}$ binding energies, respectively, are generally similar to that of dominated Cu(II) oxide species (Figure 7d).[27] However, a 0.3 eV higher in 2p binding energies is probably attributed to the presence of trace of $Cu(OH)_2$ in the film (see Figure S20 in the Supporting Information).[28] A peak at 531.3 eV was proposed to be O 1s on the surface of the film (see Figure S21 in the Supporting Information). These data reveal that electrolysis of water-soluble $[Cu(TEOA)(H_2O)_2][SO_4]$ complex in high pH aqueous solutions yields an amorphous copper oxide.

A plenty of WOCs with structural analogues to that of $CaMn_4O_5$ cluster in PSII have been reported. These catalysts could self-assemble from aqueous solution to form oxidation of metal salts[9A,25,26] or simply prepared using metal complexes[22−24] as catalyst precursors under electrolysis or illumination condition. The self-assembly of Cu(II) ions and TEOA in aqueous solution is essential to form a water-soluble Cu-based complex, thereby avoiding the precipitation of inactive $Cu(OH)_2$ in buffer solution at high pH values. Upon

DOI: 10.1021/acs.inorgchem.5b00266
Inorg. Chem. 2015, 54, 3061−3067

bulk electrolysis of the complex, single oxidation wave at 0.97 V originating from TEOA means that ligand was oxidized first, the simultaneous decomplexation of Cu-based complex and electrodeposition of CuO metal ions at ITO electrode were accompanied, and subsequent anodized to higher-valent species generating O_2. It is noteworthy that the film could form both in proton-accepting and non-proton-accepting electrolytes. In view of practical application, the long-term stability and high efficiency of the catalysts are primary requirements. In the context, Lin[14a] and Meyer[13] have reported two different Cu-based heterogeneous catalysts: the former is a coordination polymer that redissolved rapidly during electrolysis, and the latter is a surface-bound solid is formed at high initial Cu(II) salt concentration (>2.0 mM), and also redissolved into the electrolyte within 10−15 min. In the present work, the CuO film could be obtained at relatively low $[Cu(TEOA)(H_2O)_2][SO_4]$ concentrations (0.5 mM). Repeated CV scanning and extended bulk electrolysis verified the stability of the CuO film. A Faradaic efficiency of almost 100% was achieved by ITO-electrode-loaded CuO film. The overpotential of 550 mV is lower than that of previously reported homogeneous Cu-based catalysts[11−13] and may be of utility to photoelectrochemical applications.

CONCLUSION

In conclusion, we report here a robust heterogeneous CuO-based electrocatalytic system for water oxidation that can be established by electrodeposition on an electrode from a water-soluble catalyst precursor $[Cu(TEOA)(H_2O)_2][SO_4]$, which is favorable to avoid generation of $Cu(OH)_2$ precipitation in basic solution, and expand the scope for choice of electrolyte. The facile synthesis of catalyst precursor, inexpensive materials and impressive performance toward water oxidation displayed in this system are motivating for this as a new avenue of development in water oxidation catalytic system.

ASSOCIATED CONTENT

Supporting Information

Schematic diagram of experimental setup; X-ray crystallographic data for $[Cu(TEOA)(H_2O)_2][SO_4]$ in CIF format; electrochemical studies; diffuse reflectance spectra, powder X-ray diffraction patterns and energy dispersive X-ray spectroscopy of the film; the XPS spectrum centered on the Cu $2p_{3/2}$ and O 1s peaks. These material are available free of charge via the Internet at http://pubs.acs.org.

AUTHOR INFORMATION

Corresponding Author

*E-mail: fuwf@mail.ipc.ac.cn.

Notes

The authors declare no competing financial interest.

ACKNOWLEDGMENTS

This work was supported by the National Key Basic Research Program of China (973 Program No. 2013CB834804) and by the Ministry of Science and Technology of China (No. 2012DFH40090). We thank the Natural Science Foundation of China (NSFC Grant Nos. 21273257, 21471155, 21267025, and U1137606) and the Key Research Programme of the Chinese Academy of Science (Grant No. KGZD-EW-T05) for financial support.

REFERENCES

(1) (a) Crabtree, G. W.; Dresselhaus, M. S.; Buchanan, M. V. *Phys. Today* **2004**, *57*, 39. (b) Dresselhaus, M. S.; Thomas, I. L. *Nature* **2001**, *414*, 332. (c) Lewis, N. S.; Nocera, D. G. *Proc. Natl. Acad. Sci. U.S.A.* **2006**, *103*, 15729. (d) Youngblood, W. J.; Lee, S. A.; Maeda, K.; Mallouk, T. E. *Acc. Chem. Res.* **2009**, *42*, 1966. (e) Cook, T. R.; Dogutan, D. K.; Reece, S. Y.; Surendranath, Y.; Teets, T. S.; Nocera, D. G. *Chem. Rev.* **2010**, *110*, 6474.

(2) (a) Esswein, A. J.; Nocera, D. G. *Chem. Rev.* **2007**, *107*, 4022. (b) Kanan, M. W.; Surendranath, Y.; Nocera, D. G. *Chem. Soc. Rev.* **2009**, *38*, 109. (c) *Solar Hydrogen Generation*; Rajeshwar, K., McConnell, R. D., Licht, S., Eds.; Springer: New York, 2008. (d) Bard, A. J.; Fox, M. A. *Acc. Chem. Res.* **1995**, *28*, 141.

(3) (a) Barber, J. *Chem. Soc. Rev.* **2009**, *38*, 185. (b) Dempsey, J. L.; Esswein, A. J.; Manke, D. R.; Rosenthal, J.; Soper, J. D.; Nocera, D. G. *Inorg. Chem.* **2005**, *44*, 6879. (c) Dempsey, J. L.; Brunschwig, B. S.; Winkler, J. R.; Gray, H. B. *Acc. Chem. Res.* **2009**, *42*, 1995.

(4) (a) Loll, B.; Kern, J.; Saenger, W.; Zouni, A.; Biesiadka, J. *Nature* **2005**, *438*, 1040. (b) Ferreira, K. N.; Iverson, T. M.; Maghlaoui, K.; Barber, J.; Iwata, S. *Science* **2004**, *303*, 1831. (c) Yano, J.; Kern, J.; Sauer, K.; Latimer, M. J.; Pushkar, Y.; Biesiadka, J.; Loll, B.; Saenger, W.; Messinger, J.; Zouni, A.; Yachandra, V. K. *Science* **2006**, *314*, 821.

(5) (a) Li, T. T.; Chen, Y.; Li, F. M.; Zhao, W. L.; Wang, C. J.; Lv, X. J.; Xu, Q. Q.; Fu, W. F. *Chem.—Eur. J.* **2014**, *20*, 8054. (b) Li, T. T.; Zhao, W. L.; Chen, Y.; Li, F. M.; Wang, C. J.; Tian, Y. H.; Fu, W. F. *Chem.—Eur. J.* **2014**, *20*, 13957. (c) Borgarello, E.; Kiwi, J.; Pelizzetti, E.; Visca, M.; Grätzel, M. *J. Am. Chem. Soc.* **1981**, *103*, 6324. (d) McDaniel, N. D.; Coughlin, F. J.; Tinker, L. L.; Bernhard, S. *J. Am. Chem. Soc.* **2008**, *130*, 210. (e) Morris, N. D.; Mallouk, T. E. *J. Am. Chem. Soc.* **2002**, *124*, 11114. (f) Codolà, Z.; Cardoso, J. M. S.; Royo, B.; Costas, M.; Lloret-Fillol1, J. *Chem.—Eur. J.* **2013**, *19*, 7203. (g) Trasatti, S. *Electrochim. Acta* **1984**, *29*, 1503.

(6) (a) Jiao, F.; Frei, H. *Angew. Chem., Int. Ed.* **2009**, *48*, 1841. (b) Nakazono, T.; Parent, A. R.; Sakai, K. *Chem. Commun.* **2013**, *49*, 6325. (c) Berardi, S.; La Ganga, G.; Natali, M.; Bazzan, I.; Puntoriero, F.; Sartorel, A.; Scandola, F.; Campagna, S.; Bonchio, M. *J. Am. Chem. Soc.* **2012**, *134*, 11104.

(7) (a) Ellis, W. C.; McDaniel, N. D.; Bernhard, S.; Collins, T. J. *J. Am. Chem. Soc.* **2010**, *132*, 10990. (b) Hong, D.; Mandal, S.; Yamada, Y.; Lee, Y. M.; Nam, W.; Llobet, A.; Fukuzumi, S. *Inorg. Chem.* **2013**, *52*, 9522.

(8) (a) Zaharieva, I.; Chernev, P.; Risch, M.; Klingan, K.; Kohlhoff, M.; Fischer, A.; Dau, H. *Energy Environ. Sci.* **2012**, *5*, 7081. (b) Ashmawy, F. M.; McAuliffe, C. A.; Parish, R. D.; Tames, J. *J. Chem. Soc., Dalton Trans.* **1985**, *7*, 1391. (c) Limburg, J.; Vrettos, J. S.; Liable-Sands, L. M.; Rheingold, A. L.; Crabtree, R. H.; Brudvig, G. W. *Science* **1999**, *283*, 1524.

(9) (a) Wang, D.; Ghirlanda, G.; Allen, J. P. *J. Am. Chem. Soc.* **2014**, *136*, 10198. (b) Zhu, G.; Glass, E. N.; Zhao, C.; Lv, H.; Vickers, J. W.; Geletii, Y. V.; Musaev, D. G.; Song, J.; Hill, C. L. *Dalton Trans.* **2012**, *41*, 13043. (c) Dincă, M.; Surendranath, Y.; Nocera, D. G. *Proc. Natl. Acad. Sci. U.S.A.* **2010**, *107*, 10337. (d) Du, P.; Eisenberg, R. *Energy Environ. Sci.* **2012**, *5*, 6012.

(10) (a) Taki, M.; Itoh, S.; Fukuzumi, S. *J. Am. Chem. Soc.* **2001**, *123*, 6203. (b) Kang, P.; Bobyr, E.; XDustman, J.; Hodgson, K. O.; Hedman, B.; Solomon, E. I.; Stack, T. D. P. *Inorg. Chem.* **2010**, *49*, 11030.

(11) Zhang, M.; Chen, Z.; Kang, P.; Meyer, T. J. *J. Am. Chem. Soc.* **2013**, *135*, 2048.

(12) Barnett, S. M.; Goldberg, K. I.; Mayer, J. M. *Nat. Chem.* **2012**, *4*, 498.

(13) Chen, Z.; Meyer, T. J. *Angew. Chem., Int. Ed.* **2013**, *52*, 700.

(14) (a) Zhang, T.; Wang, C.; Liu, S.; Wang, J. L.; Lin, W. *J. Am. Chem. Soc.* **2014**, *136*, 273. (b) Gerlach, D. L.; Bhagan, S.; Cruce, A. A.; Burks, D. B.; Nieto, I.; Truong, H. T.; Kelley, S. P.; Herbst-Gervasoni, C. J.; Jernigan, K. L.; Bowman, M. K.; Shanlin, P.; Matthias, Z.; Elizabeth, T. P. *Inorg. Chem.* **2014**, *53*, 12689.

(15) Coggins, M. K.; Zhang, M.; Chen, Z.; Song, N.; Meyer, T. J. *Angew. Chem., Int. Ed.* **2014**, *53*, 12226.

DOI: 10.1021/acs.inorgchem.5b00266
Inorg. Chem. 2015, 54, 3061−3067

(16) Liu, X.; Jia, H. X.; Sun, Z. J.; Chen, H. Y.; Xu, P.; Du, P. W. *Electrochem. Commun.* **2014**, *46*, 1.
(17) Yu, F. S.; Li, F.; Zhang, B. B.; Li, H.; Sun, L. C. *ACS Catal.* **2015**, *5*, 627.
(18) (a) Sheldrick, G. M. *SHELXS 97, Program for the Solution of Crystal Structure*; University of Göttingen: Göttingen, Germany, 1997. (b) Sheldrick, G. M. *SHELXL97, Program for the Refinement of Crystal Structures*; University of Göttingen: Göttingen, Germany, 1997.
(19) Sen, B.; Dotson, R. L. *J. Inorg. Nucl. Chem.* **1970**, *32*, 2707.
(20) (a) Zhang, P. L.; Wang, M.; Yang, Y.; Yao, T. Y.; Sun, L. C. *Angew. Chem., Int. Ed.* **2014**, *126*, 14023. (b) Fisher, J. F.; Hall, J. L. *Anal. Chem.* **1962**, *34*, 1094.
(21) Patnaik, P. *Handbook of Inorganic Chemicals*; McGraw−Hill: New York, 2002.
(22) Fu, S.; Liu, Y.; Ding, Y.; Du, X.; Song, F.; Xiang, R.; Ma, B. *Chem. Commun.* **2014**, *50*, 2167.
(23) Junge, H.; Marquet, N.; Kammer, A.; Denurra, S.; Bauer, M.; Wohlrab, S.; Gartner, F.; Pohl, M. M.; Spannenberg, A.; Gladiali, S.; Beller, M. *Chem.—Eur. J.* **2012**, *18*, 12749.
(24) Chen, G.; Chen, L.; Ng, S.-M.; Man, W.-L.; Lau, T. C. *Angew. Chem., Int. Ed.* **2013**, *52*, 1789.
(25) (a) Kanan, M. W.; Nocera, D. G. *Science* **2008**, *321*, 1072. (b) Surendranath, Y.; Kanan, M. W.; Nocera, D. G. *J. Am. Chem. Soc.* **2010**, *132*, 16501.
(26) (a) Nocera, D. G. *Acc. Chem. Res.* **2012**, *45*, 767. (b) Surendranath, Y.; Dincă, M.; Nocera, D. G. *J. Am. Chem. Soc.* **2009**, *131*, 2615.
(27) (a) Moulder, J. F.; Stickle, W. F.; Sobol, P. E.; Bomben, K. D. *Handbook of X-ray Photoelectron Spectroscopy*, 2nd Edition; Chastain, J., Ed.; Perkin−Elmer Corp.: Eden Prairie, MN, 1992. (b) Durando, M.; Morrish, R.; Muscat, A. J. *J. Am. Chem. Soc.* **2008**, *130*, 16659. (c) Xu, S.; Ng, J.; Du, A. J. O.; Liu, J.; Sun, D. D. *Int. J. Hydrogen Energy* **2011**, *36*, 6538.
(28) (a) Casella, I. G.; Gatta, M. *J. Electroanal. Chem.* **2000**, *494*, 12. (b) Du, J. L.; Chen, Z. F.; Ye, S. R.; Wiley, B. J.; Meyer, T. J. *Angew. Chem., Int. Ed.* **2015**, DOI: 10.1002/anie.201408854.

DOI: 10.1021/acs.inorgchem.5b00266
Inorg. Chem. 2015, 54, 3061−3067